Science Publications

Online Journal of Engineering Sciences, 2021, 1, 1-18
www.scipublications.org/journal/index.php/ojes
DOI: 10.31586/ojes.2021.010101

Article

Virologic Microparticle Fluid Mechanics Simulation: COVID-19 Transmission in the Protected and Unprotected Conversations

Nima Norouzi[1,*]

[1] Department of energy engineering and physics, Amirkabir university of technology (Tehran polytechnic), 424 Hafez Avenue, PO Box 15875-4413, Tehran, Iran
*Correspondence: n.nima1376@gmail.com

Abstract: SARS-COV-19 is a serious respiratory infection created by a devastating coronavirus family (2019-nCoV) that has become the first global epidemic of the last one hundred years. It is a highly transmissible virus transmitted by inhalation or contact with the droplet core produced by infected people when they sneeze, cough, and speak. SARS-COV-2 transmission in the air is possible even in a confined space near the infected person. This study aimed to evaluate the effectiveness of using a shield or mask as a barrier to a patient's face against the spread of virus particles. For the present simulation, the discrete phase model (DPM) is used; Because this model allows us to study the particle's mass discretely in a fluid space with the continuous phase. Due to the choice of this model, the virus particles secreted from the patient's mouth are considered a discrete phase, and the open airflow in the computational area is considered a continuous phase. The present study uses fluent 2019R3 software to simulate the virus transmission to model the transient flows numerically. The analysis found that the masks or shields can be an effective method of protecting the participants of a conversation in the presence of an infected person.

Keywords: CFD; close communication; SARS-COV-2; COVID-19; Coronavirus

How to cite this paper : Norouzi, N. (2021). Virologic Microparticle Fluid Mechanics Simulation: COVID-19 Transmission in the Protected and Unprotected Conversations . *Online Journal of Engineering Sciences*, *1*(1). Retrieved from https://www.scipublications.com/journal/index.php/ojes/article/view/94

Received: July 12, 2021
Accepted: August 20, 2021
Published: August 21, 2021

1. Introduction

The new coronavirus is raging around the world, causing huge losses to countries worldwide, and has attracted the widespread attention of all humankind. To understand the transmission mechanism of such infectious diseases, people studied how the droplets exhaled by the human body spread the virus. Recently, researchers from the USA National Institutes of Health and the University of Pennsylvania used lasers and cameras to visualize the droplets produced by speech. The results showed that when people speak, they release a large amount of particle size. Droplet particles in the range of 20-500 μm[1,2]. Besides, in a closed, stagnant air environment, droplet cores with a particle size of 4 μm (corresponding to droplet particles about 12-21 μm at the exit) Can stay in the air for more than 8~14 min. These results are helpful to explain the phenomenon that the new coronavirus is more likely to spread in enclosed spaces. Therefore, understanding the production process of droplets and droplet nuclei (aerosols) in respiratory activities, particle size distribution, and transmission distance are of great significance and help to study disease transmission.

The atomization process is the main reason for the formation of droplets in respiratory activities[3]. Airflow atomization is the result of the interaction of high-speed airflow and relatively slow fluid. It is controlled by surface tension, viscosity, and aerodynamics and can occur in the respiratory tract. Atomization The size of the droplets formed in the process largely depends on different breathing patterns. For human breathing activities, different breathing patterns have significantly different biodynamic mechanisms [4].

Common breathing patterns, such as normal speaking, coughing is different from the airflow velocity exhaled during sneezing[5-7], the intensity of the turbulence caused by the airflow in the respiratory tract is different, resulting in a difference in the atomization process of the exhaled droplets, resulting in different numbers and particle size distributions. Foam.

According to statistics, the number and particle size of droplets produced by sneezing are much larger than those of talking and coughing[8-12]. Studies have shown that droplets undergo different degrees of evaporation after exiting until they are completely dried or evaporate and condense in the air environment. When the effect reaches a balance, it becomes a "droplet nucleus" [13], and the droplet nucleus has a strong ability to carry viruses [14,15]. There are also some different opinions on the size of the droplet nucleus, which is different from the droplet nucleus. The composition, initial size, and environmental conditions of the product are closely related [16,17].

The evaporation process of droplets and the size of droplet nuclei determine their movement and spread in the room[18-24]. Larger droplet particles settle quickly and are inhaled or touched by susceptible people within a short distance, namely It is "droplet propagation"; smaller droplet particles evaporate into "droplet nuclei" and move long distances with the airflow, which is called "aerosol propagation" (sometimes called "air propagation"). Understanding these modes of propagation is helpful To formulate targeted infectious disease prevention measures to guide engineering control and public health prevention.

This article aims to study the human body's exhaled droplets and droplet nuclei in virus transmission and supplements the real-time research on the virus particle size, droplet nucleus particle size, and possible transmission distance of the new coronavirus in real-time talking between two people with and without protection[25-27].

2. Theoretical Framework

2.1. Particle size distribution

The size of the particle size has an important impact on the movement and spread of droplets and further affects infectious diseases. Therefore, accurate measurement of the particle size distribution of droplets is very important for designing the ventilation system and controlling infection control. Many documents provide relevant data, but the results are not completely consistent due to different measurement methods. It is believed that droplets with a diameter of less than 5 μm are small droplets, and droplets with a diameter greater than 5 μm are large droplets[16]. This paper selects documents with detailed particle size distribution [8-12] to compare the results.

2.1.1. Talking and coughing

Studies have found that there is no significant difference in the particle size distribution between talking and coughing. Among the droplets produced by talking, about 82% have a particle size smaller than 100 μm, 37% smaller than 50 μm, and 3% smaller than 20 μm. Droplets from coughing Among the particles, the proportions of the corresponding sizes are 64%, 20%, 2.5%, and 1.4% smaller than 10 μm, and the proportion of droplets larger than 500 μm is higher when talking. This is due to the droplets generated by speech and cough. The mechanism is different; the droplet size produced by coughing is larger than the droplet size produced by speaking[27-33].

Besides, the collection method, the intensity of breathing activity, and different types of food dyes will affect the secretion of saliva, affecting the droplet size. For example, for the droplets produced when speaking, Duguid[8] and In the study of ref. 9, there are a lot of small droplets. This is due to differences in the collection methods of different documents. Their sampling points are not located at the origin (mouth) of droplets generation. Vaporization of varying degrees; Ref. 10 researched that there are more large-size droplets.

This is because the edible dyes taken by the subjects when the droplets are collected will greatly slow down the evaporation of droplets. For coughing, The results of different studies are different because the health status of the subjects and the intensity of respiratory activity are different. If it is a healthy person, it is difficult to produce a violent cough. Generally speaking, these factors are difficult to control and quantify[33-41].

2.1.2. Sneezes

Ref. 11 collected the droplets produced by 44 sneezes from 20 subjects and found two distinct particle size distributions through measurement: unimodal and bimodal. The bimodal particle size The distribution is similar to the previous study by Duguid [8]. The peak value is in the 74-86 μm particle size range, accounting for 30%; however, the unimodal particle size distribution peaks in the 340~400 μm particle size range, higher than the particle size range 340-400 μm. Duguid[8] 's research results are much larger. This is because the biodynamic mechanism of sneezing is significantly different from other respiratory activities. The initial velocity of the airflow exhaled during sneezing is about 30~100 m/s[5-7], which is far away. It is much larger than the initial air velocity of talking and coughing. Therefore, according to the atomization mechanism of droplets in the respiratory tract, the number and particle size of the droplets produced by sneezing will be much larger than the droplets produced by talking and coughing. Moreover, Ref. 8 The research time is relatively long, and the possibility that the data is not comprehensive due to limited measurement technology cannot be ruled out. Therefore, the existence of unimodal size distribution is reasonable[42-48].

Based on the above analysis, we summarized the number and main particle size range of droplet particles under different respiratory activities, and the results are shown in Table 1.

Table 1. Size of droplets under different respiratory activities

Breathing activity	Initial speed (m/s)	Total particle size	Main particle size range (μm)
speak	~5	95-755	15-55
cough	9-18	1105-2005	70-105
sneeze	27-102	2995-4995	75-350

2.2. Critical dimensions

The concept that respiratory infectious diseases are spread by droplet particles containing a certain viral load originated from ref. 18. The pathogen is released from the infected person's body, attached to the droplet particles, and discharged with the exhaled air flow and different respiratory activities. The initial velocities of the droplets are different, resulting in different propagation laws of droplets. In the study of air propagation, Ref. 13 used a simple calculation method to obtain a classic evaporation-sedimentation curve, revealing the droplet evaporation and particle size The relationship between size and sedimentation velocity, and for the first time identified the two main ways for the virus to spread by droplets. Larger droplets settle in the air quickly and move shorter horizontal distances when they land. Infections caused by inhalation or contact by susceptible people within a short distance are commonly referred to as "droplet transmission." Surgical masks significantly affect filtering large droplets [28], so you can prevent flying by wearing a mask. Spreading[49-54]. Smaller droplet particles evaporate quickly until they are completely dried, or the evaporation and condensation in the air environment reach a balance, which becomes a "droplet nucleus." In the process of droplet particle dispersion, pathogens are deposited After the droplet particles become droplet nuclei, they can stay in the air for a long period and be widely dispersed by the airflow movement.

This is the so-called "aerosol." This virus-carrying droplet After the long-distance movement of nuclear aerosol spreads, the infection caused by inhalation or contact by susceptible people is commonly referred to as "aerosol transmission" (also known as "air transmission"). Therefore, the two cores related to disease transmission are the particle size of the larger droplet and the smaller droplet? How far can the larger droplet move horizontally?

Ref. 13 first defined "larger droplets" as droplets with a particle size greater than 100 μm, which settle within a horizontal distance of 2 m; that is, droplets cause droplet propagation with a particle size greater than 100 μm. But Wells' classic research is based on simple predictions based on various physical assumptions, without considering environmental conditions and droplet composition. In the following decades, the concept of large droplets and air transmission has been extended; the particle size that distinguishes droplet transmission and air transmission is defined as the "critical size." Research has found that the critical size is a function of many physical parameters, such as environmental humidity, air velocity, and ambient temperature. This article will cause droplet transmission to cause infection. The farthest horizontal distance is called "critical distance." Both critical size and critical distance are closely related to the evaporation process of droplets[55-61].

3. Materials and Methods

The computational fluid dynamics method is used to solve the non-steady incompressible Reynolds average N-S equation [22], and the flow field of the face-to-face breathing droplet propagation area of the patient and the healthy person is obtained. The finite volume method is used to discretize the control equations, the second-order upwind-style discrete momentum equation, turbulent kinetic energy, and turbulent dissipation rate terms are used, the pressure equation is discretized in a second-order center scheme, and the coupling of velocity and pressure is coupled with the SIMPLE method[29]. The Euler model of multiphase flow [30-34] describes the two-phase flow of breathing droplets following air. The continuity equation of air and droplets is expressed by equation (1):

$$\frac{\partial(\alpha_k \rho_k)}{\partial t} + \nabla \cdot (\alpha_k \rho_k U_k) = 0 \quad (1)$$

Among them, α is the volume fraction; U is the velocity vector, m/s; the subscript k represents a certain phase, the air phase is represented by the subscript a, and the subscript d represents the droplet phase; ρ is the density, kg/m^3, air and The density and viscosity of droplets are kept constant. The momentum equation of air is expressed by equation (2)[35-37]:

$$\frac{\partial(\alpha_a \rho_a U_a)}{\partial t} + \nabla \cdot (\alpha_a \rho_a U_a U_a) = -\alpha_a \nabla p + \nabla . \tau_a + \alpha_a \rho_a g + K(U_d - U_a) \quad (2)$$

The momentum equation of droplets is expressed by equation (3):

$$\frac{\partial(\alpha_d \rho_d U_d)}{\partial t} + \nabla \cdot (\alpha_d \rho_d U_d U_d) = -\alpha_d \nabla p + \nabla \cdot \tau_d + \alpha_d \rho_d g + K(U_a - U_d) \quad (3)$$

Among them, p is the pressure of the flow field, Pa; τ is the stress tensor; g is the acceleration of gravity, m/s^2; K is the momentum exchange coefficient between the air and droplet phases.

The RNG k-ε turbulence model has a wide range of adaptability. It can simulate high Reynolds number flow and the viscosity analytical formula of low Reynolds number flow in the turbulence model. Literature [38] shows that the turbulence model can simulate indoor airflow organization. Has a good effect. Therefore, this paper uses the RNG k-ε

turbulence model to describe the turbulent flow [39, 61-65] and uses the wall function method to connect the physical quantities near the wall with the unknown quantities in the turbulent core area. The dimensionless distance between the node closest to the wall and the wall satisfies 30≤ y+≤300[27-29]. Use the following form to describe the turbulence model equation:

$$\frac{\partial(\rho\phi_k)}{\partial t} + \nabla \cdot (\rho U_k \phi_k - \Gamma\phi_k grad\phi_k) = S\phi_k, k = 1, \ldots, N \quad (4)$$

Where ϕk is a scalar; Γϕk is the diffusion coefficient; Sϕk is the source term of the Nth scalar equation. The structural grid technology and the H-shaped grid topology are used to divide the calculation area. Right-angle grids are used throughout the venue to ensure the orthogonality of the near-wall grids and the accuracy of the calculation results. The droplet inlet adopts the given velocity inlet condition; not only the jet velocity is given, but also the turbulence parameters, including turbulence intensity and turbulence viscosity ratio, are described by the following equations [40-42]:

$$u = Vcos\theta, v = Vsin\theta \quad (5)$$

$$C_d = Csin(2\pi t) \quad (6)$$

$$I = \frac{u'}{V} = 3\% \quad (7)$$

$$\sigma = \frac{\mu_t}{\mu} = 10 \quad (8)$$

Among them, V is the droplet ejection velocity at the inlet, u and v are the velocity components in the X and Y directions respectively, m/s; θ is the droplet ejection angle, °; C is the peak droplet concentration at the inlet; Cd is the flow field Droplet concentration in mg/m3; t is the flow time, s; u′ is the root mean square of the velocity fluctuation, m/s; I is the turbulence intensity; σ is the turbulence viscosity ratio; turbulence intensity, turbulence viscosity ratio They are given as 3% and 10 respectively, and medium turbulence intensity values are used[41].

The exit boundary adopts the condition that the normal gradient of the flow variable is zero. At the same time, the turbulence intensity of the outlet, the turbulence viscosity ratio, and other parameters all adopt the given value of the inlet boundary. The boundary conditions are based on the ref. [16]. Since this article is studying the flow and propagation of face-to-face droplets in an open space, the outlets are set above the heads of healthy people and patients and The top of the entire calculation area. If the calculation area is a narrow space in the elevator, the top of the calculation area should be set as a fixed wall, and the top of the head of healthy people and patients should still be set as an exit. The patient, healthy person, anti-droplet mask, and the ground all adopt solid-wall boundary conditions. The anti-droplet mask is divided into the inner, outer surface, and top, and the fixed-wall boundary adopts speed and non-slip conditions. The initial conditions use static flow parameter values; that is, all flow parameters in the initial field are zero. The relationship between the peak spray concentration of the inlet droplets and the number of droplets is expressed by the following equation [23]:

$$M = \frac{C}{\rho\frac{1}{6}\pi d^3} \quad (9)$$

C is the peak droplet concentration at the inlet, mg/m³; M is the number of droplets per unit volume of the inlet, 1/m³; ϱ is the droplet density, kg/m³; d is the droplet diameter, m. The relationship between the peak droplet concentration at the entrance and the volume fraction [23] is as follows:

$$\alpha_d = C_\rho \tag{10}$$

Among them, αd is the droplet volume fraction, representing the volume ratio of droplets per unit volume; the subscript d represents droplets. This article focuses on horizontal transmission lines (0≤X≤2 m, Y = 1.5 m), vertical transmission lines (X = 1.95 m, 0≤Y≤2.8 m), and a healthy human nose and mouth (X = 2 m, 1.5 m≤ Y≤1.52 m) droplet concentration analysis. This article ignores the phase transition problem of breathing droplets.

4. Results

4.1. Unprotected case scenario

Coronavirus (covid 19) is the biggest human challenge today, and the high transmission rate of this disease is very problematic. One of the important advice of doctors regarding preventing the transmission of the disease between people is to maintain social distance between people when talking to each other. In this project, based on the CFD method and using Ansys fluent software, an attempt has been made to simulate the release of virus particles from the mouth of a coronary carrier patient while talking and transmitting it to another person in a certain space. This study investigates the ability of virus particles to propagate and transmit at a distance less than social distance. For the present simulation, the discrete phase model (DPM) is used; Because this model allows us to study a mass of particles discretely or bit by bit in a continuously fluid space. Due to the choice of this model, the virus particles secreted from the patient's mouth are considered a discrete phase, and the open airflow in the computational area is considered a continuous phase. The type of discrete phase behavior will be time-dependent and with a time step of 0.001 s (activating the unsteady particle tracking mode). After activating the discrete phase model, the injection process must be defined, determining the type and quality of discrete particles injected into the model. In this model, the emitted particles are defined as the inert type, and the injection type is the surface and is done through the surface of the patient's mouth. These virus particles have a constant diameter of 0.000001 m and a temperature of 310 K, which are spread between 0 s and 20 s. A specific profile has been used to define the velocity and discharge of virus particles exiting the corona mouth. This profile shows the amount of velocity and flow of particles emitted when speaking; Thus, these virus particles are removed from the patient's mouth in a time-dependent manner. The particle velocity profile is defined as a sinusoidal function with a maximum velocity of 0.33 m.s-1, and the particle flow rate is defined by a specific ratio to the particle velocity. Also, the boundary conditions related to the discrete phase model have been defined in such a way that particles at the boundary of the patient's mouth have an escaped state, meaning particles pass through this boundary and at the boundaries of both the body and the floor have a trap state meaning Particles are trapped and accumulate at these boundaries. The present simulation process has been performed unstable for 40 s with a time step equal to 0.05 s. The present model is designed in three dimensions using design modeler software. The model's geometry includes a computational space with dimensions of 1.6 meters * 2 meters * 2.6 meters in which two people are facing each other at a distance of 80 cm from each other. One of these two people is designed as a patient; So that the patient's mouth is defined as the source of the spread of the virus caused by talking. Hence, the patient's human mouth level is differentiated by the Mouth boundary condition; Because this level is assumed as the reference level of discrete phase virus release in this model(See Figure 1).

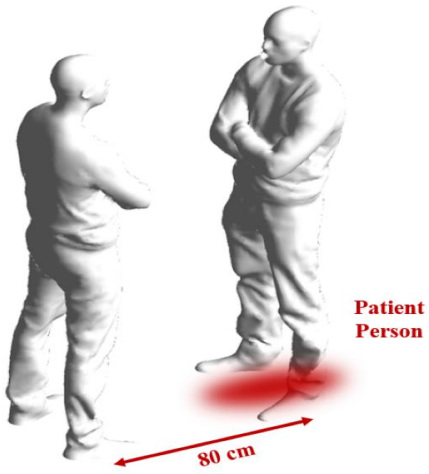

Figure 1. Schematics of system

Networking is done in three dimensions using Ansys meshing software. Networking is done without organization, and the number of cells produced in this modeling is equal to 724076(See Figure 2).

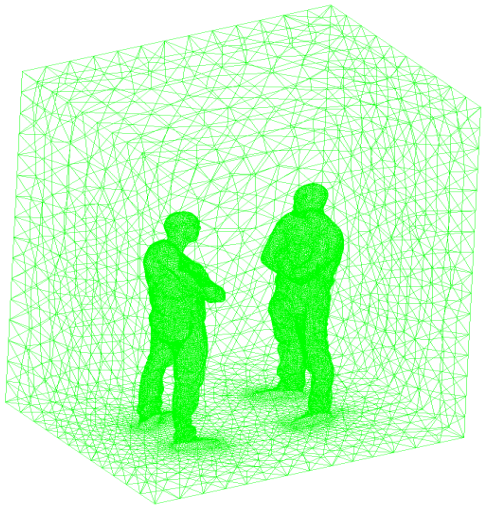

Figure 2. Meshing schematics

To simulate the present model, several assumptions have been considered, which are:

- Pressure-based simulation has been performed.
- Simulations have been performed in both fluid and heat transfer modes.
- The present model is temporally unsteady; Because the purpose of the problem is to follow the particles related to the discrete phase over time.
- The effect of gravity on the fluid is 9.81m.s^{-2} and is considered along the z-axis.

At the end of the resolution process, particle tracking of the virus particles at different time intervals was obtained from the simulation process. This particle sequence is based on the residence time of the particles and the amount of velocity of the particles. As can be seen from the images, and according to the defined simulation process, the virus particles are expelled from the carrier's mouth in waves for the first 20 seconds, and only the particles in the space between the second 20 seconds. The carrier and healthy person continue to move. According to the results, it can be concluded that by talking to the patient

for 20 seconds, these virus particles are transmitted to a healthy person after 40 seconds and expose to receiving virus particles (See Figure 3 and Figure 4).

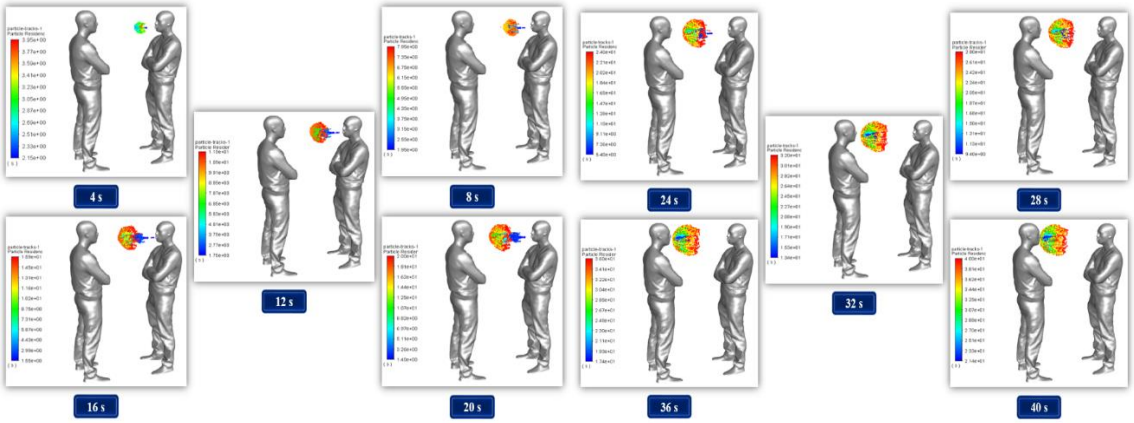

Figure 3. Particle reside in first 40s after the starting conversation

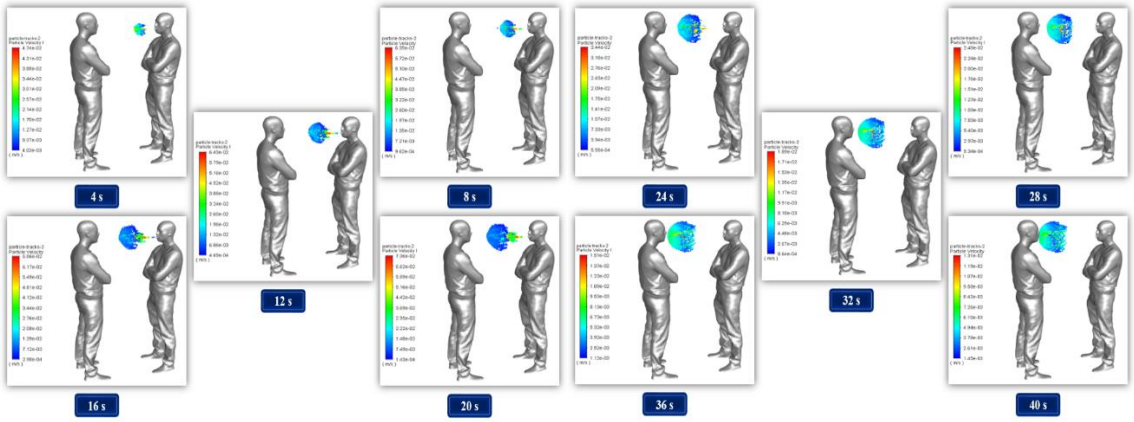

Figure 4. Particle velocity in first 40s after the starting conversation

4.2 protected case scenario

Coronavirus (covid 19) is the biggest human challenge today, and the high transmission rate of this disease is very problematic. One of the important doctors' recommendations regarding preventing disease transmission between people is using special masks or shields at low social distances. In this project, based on the CFD method and using Ansys fluent software, an attempt has been made to simulate the release of virus particles from the mouth of a coronary carrier patient while talking and to prevent their transmission to another person using a shield. . this study aimed to evaluate the effectiveness of using a shield or mask as a barrier on the face of a virus carrier against the spread of virus particles. For the present simulation, the discrete phase model (DPM) is used; Because this model allows us to study a mass of particles discretely or bit by bit in a continuously fluid space. Due to the choice of this model, the virus particles secreted from the patient's mouth are considered a discrete phase, and the open airflow in the computational area is considered a continuous phase. The type of discrete phase behavior will be time-dependent and with a time step of 0.001 s (activating the unsteady particle tracking mode). After activating the discrete phase model, the injection process must be defined, determining the type and quality of discrete particles injected into the model. In this model, the emitted particles are defined as the inert type, and the injection type is the surface and is done through the surface of the patient's mouth. These virus particles have a fixed diameter of 0.000001 meters and a temperature of 310 Kelvin, which propagate throughout 0 to 20 seconds. A

specific profile has been used to define the velocity and discharge of virus particles exiting the corona mouth. This profile shows the amount of velocity and flow of particles emitted when speaking; Thus, these virus particles are removed from the patient's mouth in a time-dependent manner. The particle velocity profile is defined as a sinusoidal function with a maximum velocity of 0.33 m / s, and the particle flow rate is defined by a specific ratio to the particle velocity. Also, the boundary conditions related to the discrete phase model are defined in such a way that particles at the boundary of the patient's mouth have an escaped state, meaning that the particles cross this boundary, and at the boundaries of both the body and the floor, as well as the surface. Masks or shields mounted on the patient's face have a trap mode, which means that particles are trapped and accumulate in these borders. The present simulation process is performed unstable and in a time interval of 40 seconds with a time step equal to 0.05 seconds.

The present model is designed in three dimensions using design modeler software. The model's geometry includes a computational space with dimensions of 1.6 meters * 2 meters * 2.6 meters in which two humans are facing each other at a distance of 80 cm from each other. One of these two people is designed as a patient; So that the patient's mouth is defined as the source of the spread of the virus caused by talking. Hence, the patient's human mouth level is differentiated by the Mouth boundary condition; Because this level is assumed as the reference level of discrete phase virus release in this model. On the other hand, a shield number is depicted as a barrier on the face of the same person carrying the virus(See Figure 5).

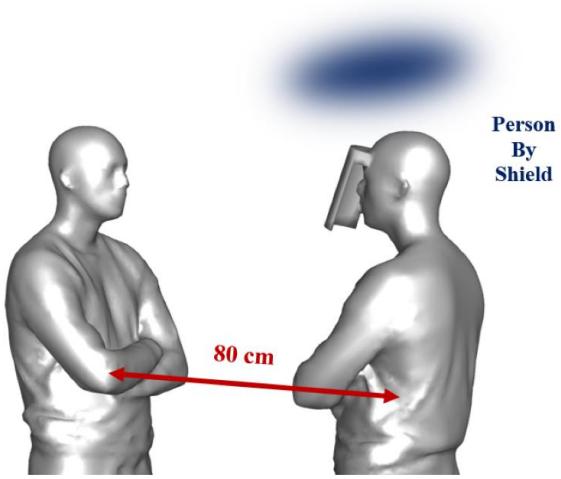

Figure 5. Schematics of case 2

Networking is done in three dimensions using Ansys meshing software. Networking is done without organization, and the number of cells produced in this modeling is equal to 724043(See Figure 6).

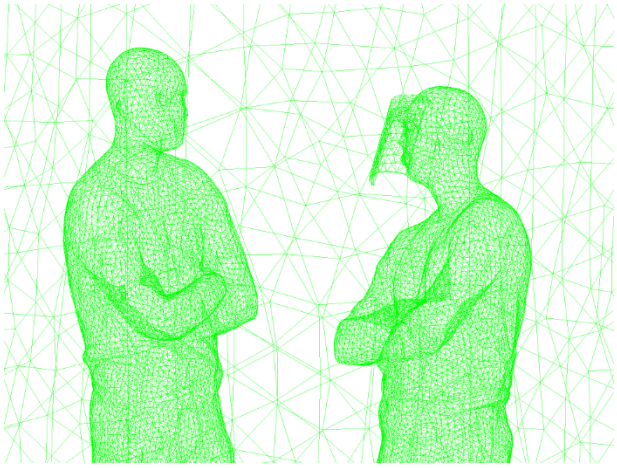

Figure 6. The meshing network of case 2

At the end of the resolution process, particle tracking of the virus particles at different time intervals was obtained from the simulation process. This particle sequence is based on the residence time of the particles and the amount of velocity of the particles. As can be seen from the images, and according to the simulation process defined, the virus particles are expelled in waves from the carrier's mouth in 20 s. According to the pictures, it can be concluded that the presence of a shield causes the virus particles to come out of the patient's mouth to accumulate on the shield and not be transmitted to a healthy person(See Figure 7 and Figure 8).

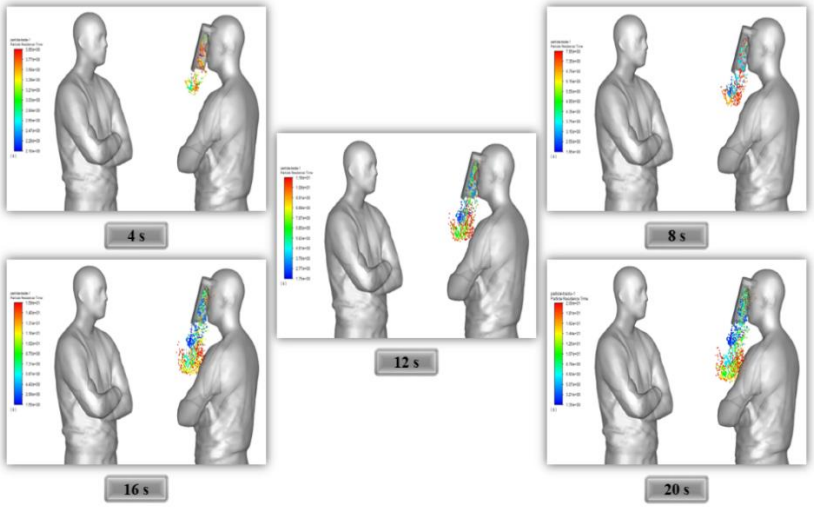

Figure 7. Particle reside in first 40s after the starting conversation in the presence of a shield

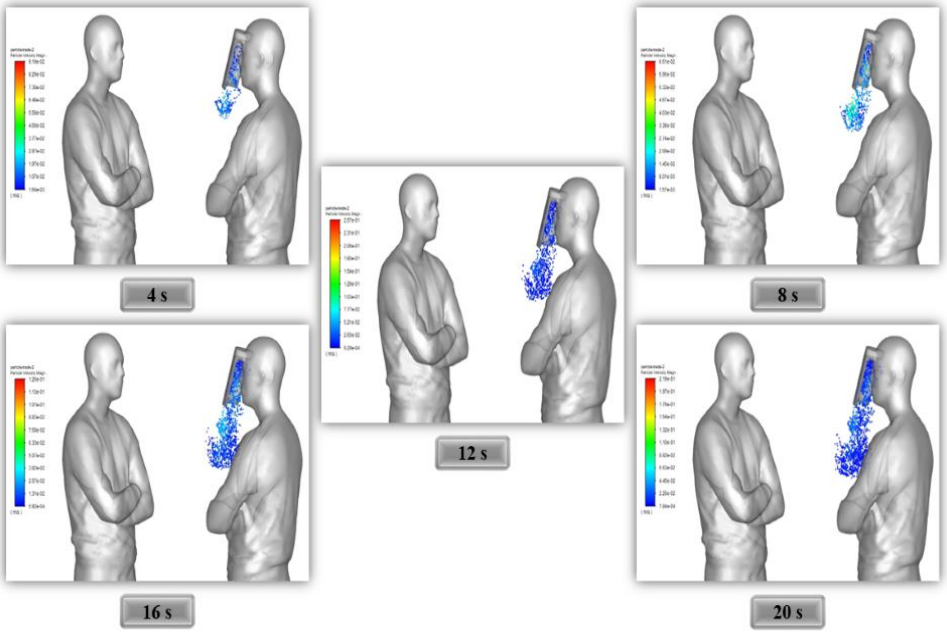

Figure 8. Particle velocity in first 40s after the starting conversation in the presence of a shield

4. Discussion

4.1. Droplet evaporation and its influencing factors

In the process of droplet particles evaporating into droplet nuclei, especially when they are close to the dry state, the mortality of pathogens in the particles increases greatly, and the degree of increase depends on the type of pathogens[14,15]. Although large droplets carry pathogens Has a stronger ability, their ability to penetrate the respiratory tract is lower than that of small droplets. In general, small droplets (diameter <5 μm) are more infectious than large droplets[16,17,29]. It is generally believed that The particle size of the droplet nucleus is 1~3 μm[19,20], mainly concentrated in the range of less than 1 μm. Ref. 30 measured the influenza virus concentration in a health center and on an airplane and found that it was carrying the virus 64% of the droplet nuclei have a particle size of fewer than 2.5 μm. Therefore, the evaporation process is a key factor in the spread of the virus, which is significantly related to the relative humidity (RH) of the ambient air and the initial size of the droplet.

4.2. Relative air humidity

Due to the different concentrations of organic polymers such as proteins, lipids, and carbohydrates contained in the droplets, it is generally believed that the diameter (dr) of the droplet core is approximately 0.25 to 0.5 times the initial droplet diameter (di)[16]. Ref. 22 established a respiratory droplet equilibrium model based on the Kelvin effect. The study found that droplet particles with low protein content (3 mg/mL) have a droplet nucleus size under environmental conditions where the RH is lower than 64%. The relationship with the initial particle size remains unchanged (d_r=0.2d_i), the relationship

between the droplet core particle size and the initial particle size of droplet particles with high protein content (76 mg/mL) under environmental conditions where the RH is lower than 42% No change (dr=0.4di). When the relative air humidity of the environment is higher than these two RH values, the dr/di of the droplet particles with two kinds of protein content increase with the increase of RH. This is due to the relative humidity Air with high humidity has a lower ability to absorb water vapor, which can significantly delay the evaporation process of droplets.

4.3. Initial dimensions

The initial size is another important factor that affects the size of the droplet nucleus during the evaporation of droplets [17]. 10 μm droplets evaporate quickly (<0.1 s) and are not affected much by RH. 50 μm droplets It can completely evaporate to become a droplet nucleus before landing, and the evaporation time gradually increases with the increase of RH (about 1-10 s). The evaporation process of 100 μm droplet particles slows down significantly with the increase of RH and low RH (<30 %); most of the droplets can completely evaporate before landing and become droplet nuclei and move with the airflow. Still, at high RH (>60%), the evaporation rate is greatly reduced, and most of the droplets fall to the ground before completely evaporating. The 200 μm droplet particles settle rapidly, and the settling time increases slightly with the decrease of RH (about 1-5 s). It is worth noting that the premise of this study is to simplify the droplets produced by normal breathing to pure Water droplets. In fact, in addition to the insoluble core, droplet particles also contain sodium-potassium cations, chloride anions, lactate, glycoprotein, and other components, considering that other respiratory activities such as speaking, coughing, etc., the airflow velocity is higher than normal breathing. Therefore, the actual evaporation rate should increase, and the sedimentation rate should decrease.

To sum up, the critical size should be a range, which characterizes the transition section of droplets from completely evaporating first to falling to the ground: droplets within this particle size range can be completely evaporated in a relatively dry air environment. The droplet nucleus with a small enough particle size can cause long-distance air propagation with the movement of the airflow; it can also evaporate slowly in a relatively humid air environment and settle within a critical distance because the volume and mass are not enough to be suspended in the air Cause droplets to spread.

4.4. The role of protection

Shields, Surgical masks, and N95 masks play an important role in preventing airborne viruses [28], effectively reducing the range of exhaled jets. The effectiveness of masks to block aerosol particles depends on several factors: air velocity through the mask, droplets, particle size distribution, and the degree of air leakage around the mask. Ref. 37 visualized the airflow process of coughing droplets by the optical schlieren method. The results showed that no matter what kind of mask is worn, there is air leakage: wear In general surgical masks, the air leakage is mainly concentrated on the top and bottom of the mask; when wearing an N95 mask, although the edge leakage is significantly reduced, due to the

large pressure inside the mask, a small number of droplets are forced to pass directly through the mask and form a forward direction. After wearing a mask, the droplet momentum generated by coughing is greatly reduced, causing the horizontal distance of droplet movement to be shortened to less than 0.5 m, and the movement of these droplets mainly follows the human body. The heat plume rises instead of being deposited on the surface of susceptible people or inhaled by them. Therefore, masks still play a great role in blocking and reducing the spread of the virus.

4.5. Effects of resuspension

Ref. 21 measured the viral RNA in aerosols in different areas of two hospitals in Wuhan, and found that the aerosols containing the new coronavirus are mainly distributed in two-particle size ranges: 0.25~0.5 and 0.5~1 μm, and proposed The surface deposition and resuspension of protective clothing for medical personnel and toilets may be a way of transmission of virus aerosols. Ref. 22 measured people wearing clothes of different materials in closed spaces (cleanroom coveralls, polyester sportswear, cotton clothes), the emission of particles when performing activities of different intensities (sitting, light activities, vigorous activities), it is found that for particles with a diameter of 0.3~5 μm, the incidence of particles when wearing polyester sportswear is the highest; for those with a particle size of less than two μm For particulate matter, the activity intensity has no significant effect on the particle occurrence rate; for particles with a particle size greater than two μm, the particle occurrence rate is positively correlated with the activity intensity; moreover, the resuspension of particles from the deposition surface requires a very large momentum (wind speed). Ref. 23 and 24 summarized the deposition and resuspension of indoor particles. The study found that for particles with diameters of 0.5 and 1 μm, the average indoor sedimentation rate is 2.2×10–5 and 9.72×10–5 m/s, respectively, The corresponding resuspension rates are 2.0×10–10 and 50×10–10 s–1. It can be seen that the magnitude of the resuspension rate is much smaller than the magnitude of the corresponding average sedimentation rate. This result further confirms that there are relatively few particles resuspended on the deposition surface. Therefore, it can be considered that in the non-specialized treatment and care of infectious patients, it is impossible to deposit a large amount of virus aerosol on the surface of human clothes, and the virus aerosol is not easy to resuspend. When the ventilation conditions are good, transmission by the resuspension of droplets or droplet nuclei deposited on the surface of the human body as a medium is not the main way of air transmission. Ref. 25 observed the particle size of the novel coronavirus by a transmission electron microscope to be 0.06-0.14 μm; Bar-On et al. [26] preliminary believed that the new coronavirus is a virus with a particle size of fewer than 0.1 μm. Ref. 21 measured the viral RNA in aerosols and found that the droplet nuclei containing the new coronavirus are mainly distributed in two-particle size ranges: 0.25-0.5 and 0.5-1 μm. Ref. 27 considered the high-momentum turbulence effect when sneezing or coughing and proposed that the virus spread as far as 7-8 m. However, these conclusions are still in the discussion stage. There are still many

uncertainties. Determining the particle size range and transmission distance of the droplets carrying the new coronavirus requires more detailed research.

5. Conclusions

This paper combs and summarizes the research results of the particle size distribution, evaporation law, and transmission law of human body exhaled droplets. The main conclusions are as the main particle size ranges of droplets exhaled by normal speaking, coughing, and sneezing are 10-50, 73-100, and 80-340 μm, respectively. The critical distance between droplet propagation and air propagation is about 2.5 m. The particle size of droplet nuclei varies according to environmental conditions, droplet composition, and initial size. It is generally believed that the particle size of droplet nuclei, which greatly contributes to air transmission, is 1-3 μm, mainly Concentrated in the range of less than 1 μm. Droplets larger than 110 μm can land before moving a horizontal distance of 2.5 m, which is the prerequisite for droplet propagation; droplets smaller than 30 μm completely evaporate into droplet nuclei before landing and stay in the air for a long time It is the prerequisite for air propagation (aerosol propagation) to neutralize and move with the airflow. The movement and propagation laws of 30-110 μm droplet particles vary according to environmental conditions and initial speed.

Supplementary Materials: "Not Applicable."

Author Contributions: "Conceptualization, NN; methodology, NN; software, NN; validation, NN; formal analysis, NN; investigation, NN; resources, NN; data curation, NN; writing—original draft preparation, NN; writing—review and editing, NN; visualization, NN; supervision, NN; project administration, NN; funding acquisition, NN All authors have read and agreed to the published version of the manuscript."

Funding: "This research received no external funding."

Data Availability Statement: "Data will be available by request from the corresponding author."

Acknowledgments: "Not Applicable."

Conflicts of Interest: "The authors declare no conflict of interest."

References

[1] Chen, L.; Liu, W.; Zhang, Q.; Xu, K.; Ye, G.; Wu, W.; Sun, Z.; Liu, F.; Wu, K.; Zhong, B.; et al. RNA based mNGS approach identifies a novel human coronavirus from two individual pneumonia cases in 2019 Wuhan outbreak. Emerg. Microbes Infect. 2020, 9, 313–319.

[2] Zhou, P.; Yang, X.-L.; Wang, X.-G.; Hu, B.; Zhang, L.; Zhang, W.; Si, H.-R.; Zhu, Y.; Li, B.; Huang, C.-L.; et al. A pneumonia outbreak associated with a new coronavirus of probable bat origin. Nature 2020, 579, 270–273.

[3] World Health Organization. Infection Prevention and Control of Epidemic- and Pandemic-Prone Acute Respiratory Infections in Health Care; World Health Organization: Geneva, Switzerland, 2014.

[4] How COVID-19 Spreads. 2020. Available online: https://www.cdc.gov/coronavirus/2019-ncov/about/transmission.html (accessed on 15 January 2021).

[5] Asadi, S.; Bouvier, C.; Wexler, A.S.; Ristenpart, W.D. The coronavirus pandemic and aerosols: Does COVID-19 transmit via expiratory particles? Aerosol Sci. Technol. 2020, 6, 635–638.

[6] Liu, Y.; Ning, Z.; Chen, Y.; Guo, M.; Liu, Y.; Gali, NK.; Sun, L.; Duan, Y.; Cai, J.; Westerdahl, D.; et al. Aerodynamic characteristics and RNA concentration of SARS-CoV-2 aerosol in Wuhan hospitals during COVID-19 Outbreak. bioRxiv 2020.

[7] Tellier, R.; Li, Y.; Cowling, B.J.; Tang, J.W. Recognition of aerosol transmission of infectious agents: A commentary. BMC Infect. Dis. 2019, 19, 1–9.

[8] Jones, R.M.; Brosseau, L.M. Aerosol transmission of infectious disease. J. Occup. Environ. Med. 2015, 57, 501–508.

[9] Xie, X.; Li, Y.; Sun, H.; Liu, L. Exhaled droplets due to talking and coughing. J. R. Soc. Interface 2009, 6, S703–S714.

[10] Wei, J.; Li, Y. Airborne spread of infectious agents in the indoor environment. Am. J. Infect. Control. 2016, 44, S102–S108.

[11] Xie, X.; Li, Y.; Chwang, A.T.Y.; Ho, PL; Seto, W.H. How far droplets can move in indoor environments? revisiting the Wells evaporation-falling curve. Indoor Air 2007, 17, 211–225.

[12] van Doremalen, N.; Bushmaker, T.; Morris, D.; Holbrook, M.; Gamble, A.; Williamson, B.; Tamin, A.; Harcourt, J.; Thornburg, N.; Gerber, S.; et al. Aerosol and surface stability of SARS-CoV-2 as compared with SARS-CoV-1. N. Engl. J. Med. 2020, 1–3.

[13] Casanova, L.M.; Jeon, S.; Rutala, W.A.; Weber, D.J.; Sobsey, M.D. Effects of air temperature and relative humidity on coronavirus survival on surfaces. Appl. Environ. Microbiol. 2010, 76, 2712–2717.
[14] Kampf, G.; Todt, D.; Pfaender, S.; Steinmann, E. Persistence of coronaviruses on inanimate surfaces and their inactivation with biocidal agents. J. Hosp. Infect. 2020, 104, 246–251.
[15] Kampf, G. Potential role of inanimate surfaces for the spread of coronaviruses and their inactivation with disinfectant agents. Infect. Prev. Pr. 2020, 2, 100044.
[16] Chin, A.W.H.; Chu, J.T.S.; Perera, M.R.A.; Hui, K.P.Y.; Yen, H.-L.; Chan, M.C.W.; Peiris, M.; Poon, L.L.M. Stability of SARS-CoV-2 in different environmental conditions. Lancet 2020, 1, e10.
[17] Popa, A.; Genger, J.-W.; Nicholson, M.D.; Penz, T.; Schmid, D.; Aberle, S.W.; Agerer, B.; Lercher, A.; Endler, L.; Colaço, H.; et al. Genomic epidemiology of superspreading events in Austria reveals mutational dynamics and transmission properties of SARS-CoV-2. Sci. Trans. Med. 2020, eabe2555.
[18] Johnston, S.C.; Ricks, K.M.; Jay, A.; Raymond, J.L.; Rossi, F.; Zeng, X.; Scruggs, J.; Dyer, D.; Frick, O.; Koehler, J.W.; et al. Development of a coronavirus disease 2019 nonhuman primate model using airborne exposure. PLoS ONE 2021, 16, e0246366.
[19] Buonanno, G.; Stabile, L.; Morawska, L. Estimation of airborne viral emission: Quanta emission rate of SARS-CoV-2 for infection risk assessment. Environ. Intern. 2020, 141, 105794.
[20] Prentiss, M.G.; Chu, A.; Berggren, K.K. Superspreading events without superspreaders: Using high attack rate events to estimate No for airborne transmission of COVID-19. medRxiv 2020.
[21] Karimzadeh, S.; Bhopal, R.; Tien, H.N. Review of Infective Dose, Routes of Transmission, and Outcome of COVID-19 Caused by the SARS-CoV-2 Virus: Comparison with Other Respiratory Viruses. 2020. Available online: https://www.preprints.org (accessed on 26 February 2021).
[22] Lelieveld, J.; Helleis, F.; Borrmann, S.; Cheng, Y.; Drewnick, F.; Haug, G.; Klimach, T.; Sciare, J.; Su, H.; Pöschl, U. Model calculations of aerosol transmission and infection risk of COVID-19 in indoor environments. Int. J. Environ. Res. Public Health 2020, 17, 8114.
[23] Bredberg, A.; Gobom, J.; Almstrand, A.-C.; Larsson, P.; Blennow, K.; Olin, A.-C.; Mirgorodskaya, E. Exhaled endogenous particles contain lung proteins. Clin. Chem. 2012, 58, 431–440.
[24] Alsved, M.; Matamis, A.; Bohlin, R.; Richter, M.; Bengtsson, P.E.; Fraenkel, C.J.; Medstrand, P.; Löndahl, J. Exhaled respiratory particles during singing and talking. Aerosol Sci. Technol. 2020, 54, 1245–1248.
[25] Wilson, N.M.; Norton, A.; Young, F.P.; Collins, D.W. Airborne transmission of severe acute respiratory syndrome coronavirus-2 to healthcare workers: A narrative review. Anaesthesia 2020, 75, 1086–1095.
[26] Almstrand, A.-C.; Bake, B.; Ljungström, E.; Larsson, P.; Bredberg, A.; Mirgorodskaya, E.; Olin, A.-C. Effect of airway opening on production of exhaled particles. J. Appl. Physiol. 2010, 108, 584–588.
[27] Wells, F.W. Airborne Contagion and Air Hygiene. An Ecological Study of Droplet Infections; Harvard University Press: Cambridge, UK, 1955; p. 423.
[28] Walker, J.S.; Archer, J.; Gregson, F.K.; Michel, S.E.; Bzdek, B.R.; Reid, J.P. Accurate representations of the microphysical processes occurring during the transport of exhaled aerosols and droplets. ACS Cent. Sci. 2021, 7, 200–209.
[29] Hussein, T.; Löndahl, J.; Paasonen, P.; Koivisto, A.J.; Petäjä, T.; Hämeri, K.; Kulmala, M. Modeling regional deposited dose of submicron aerosol particles. Sci. Total. Environ. 2013, 458–460, 140–149.
[30] Hussein, T.; Kulmala, M. Indoor aerosol modeling: Basic principles and practical applications. Water Air Soil Pollut. Focus 2007, 8, 23–34.
[31] Nazaroff, WW Indoor Particle Dynamics. Indoor Air 2004, 14, 175–183.
[32] Holmes, J.R. How Much Air do We Breath? California Environmental Protection Agency: Sacramento, CA, USA, 1994.
[33] ICRP. Annals of the International Commission on Radiological Protection ICRP Publication 66: Human Respiratory Tract Model. for Radiological Protection; International Commission on Radiological Protection: Ottawa, ON, Canada, 1994.
[34] Anjilvel, S.; Asgharian, B. A multiple-path model of particle deposition in the rat lung. Toxicol. Sci. 1995, 28, 41–50.
[35] Löndahl, J.; Massling, A.; Pagels, J.; Swietlicki, E.; Vaclavik, E.; Loft, S. Size-resolved respiratory-tract deposition of fine and ultrafine hydrophobic and hygroscopic aerosol particles during rest and exercise. Inhal. Toxicol. 2007, 19, 109–116.
[36] Xu, Q.; Fan, QY; Duan, N.; Wang, W.; Chen, J.H. Air-borne spread pathway in intensive care unit (ICU) of specialized SARS hospital. Chin. J. Nosoconmiol. 2005, 15, 1380–1382.
[37] Alsved, M.; Fraenkel, C.-J.; Bohgard, M.; Widell, A.; Söderlund-Strand, A.; Lanbeck, P.; Holmdahl, T.; Isaxon, C.; Gudmundsson, A.; Medstrand, P.; et al. Sources of airborne norovirus in hospital outbreaks. Clin. Infect. Dis. 2020, 70, 2023–2028.
[38] Wells, W.F. On air-borne infection—Study II droplets and droplet nuclei. Am. J. Epidemiol. 1934, 20, 611–618.
[39] LeClair, JM; Zaia, J.A.; Levin, M.J.; Congdon, R.G.; Goldmann, D.A. Airborne transmission of chickenpox in a hospital. N. Engl. J. Med. 1980, 302, 450–453.
[40] Garner, J.S. Hospital infection control practices advisory committee guideline for isolation precautions in hospitals. Infect. Control. Hosp. Epidemiol. 1996, 17, 53–80.
[41] Escombe, A.R.; Oeser, C.; Gilman, R.H.; Navincopa, M.; Ticona, E.; Martínez, C.; Caviedes, L.; Sheen, P.; Gonzalez, A.; Noakes, C.; et al. The detection of airborne transmission of tuberculosis from HIV-infected patients, using an in vivo air sampling model. Clin. Infect. Dis. 2007, 44, 1349–1357.

[42] Wan, M.P.; Chao, C.Y.H.; Chao, Y.H.C. Transport characteristics of expiratory droplets and droplet nuclei in indoor environments with different ventilation airflow patterns. J. Biomech. Eng. 2006, 129, 341–353.
[43] Li, Y.; Huang, X.; Yu, I.T.S.; Wong, T.W.; Qian, H. Role of air distribution in SARS transmission during the largest nosocomial outbreak in Hong Kong. Indoor Air 2005, 15, 83–95.
[44] Xiao, S.; Li, Y.; Wong, T.-W.; Hui, D.S.C. Role of fomites in SARS transmission during the largest hospital outbreak in Hong Kong. PLoS ONE 2017, 12, e0181558.
[45] Yan, R.; Zhang, Y.; Guo, Y.; Xia, L.; Zhou, Q. Structural basis for the recognition of the 2019-nCoV by human ACE2. bioRxiv 2020.
[46] Booth, T.F.; Kournikakis, B.; Bastien, N.; Ho, J.; Kobasa, D.; Stadnyk, L.; Li, Y.; Spence, M.; Paton, S.; Henry, B.; et al. Detection of airborne severe acute respiratory syndrome (SARS) coronavirus and environmental contamination in SARS outbreak units. J. Infect. Dis. 2005, 191, 1472–1477.
[47] Olsen, S.J.; Chang, H.-L.; Cheung, T.Y.-Y.; Tang, A.F.-Y.; Fisk, T.L.; Ooi, S.P.-L.; Kuo, H.-W.; Jiang, D.D.-S.; Chen, K.-T.; Lando, J.; et al. Transmission of the severe acute respiratory syndrome on aircraft. N. Engl. J. Med. 2003, 349, 2416–2422.
[48] Fineberg, H.V. Rapid Expert Consultation on the Possibility of Bioaerosol Spread of SARS-CoV-2 for the COVID-19 Pandemic; The National Academies Press: Washington, DC, USA, 2020.
[49] Is the Coronavirus Airborne? Experts Can't Agree. Nature News. 2020. Available online: https://www.nature.com/articles/d41586-020-00974-w (accessed on 3 January 2021).
[50] Qian, H.; Zheng, X. Ventilation control for airborne transmission of human exhaled bio-aerosols in buildings. J. Thorac. Dis. 2018, 10, S2295–S2304.
[51] Kleiboeker, S.; Cowden, S.; Grantham, J.; Nutt, J.; Tyler, A.; Berg, A.; Altrich, M. SARS-CoV-2 viral load assessment in respiratory samples. J. Clinical Virol. 2020, 129, 104439.
[52] van Kampen, J.J.; van de Vijver, D.A.; Fraaij, P.L.; Haagmans, B.L.; Lamers, M.M.; Okba, N.; van den Akker, J.P.; Endeman, H.; Gommers, D.A.; Cornelissen, J.J.; et al. Duration and key determinants of infectious virus shedding in hospitalized patients with coronavirus disease-2019 (COVID-19). Nat. Commun. 2021, 12, 1–6.
[53] Gregson, F.K.A.; Watson, N.A.; Orton, C.M.; Haddrell, A.E.; McCarthy, L.P.; Finnie, T.J.R.; Gent, N.; Donaldson, G.C.; Shah, P.L.; Calder, J.D.; et al. Comparing aerosol concentrations and particle size distributions generated by singing, speaking and breathing. Aerosol Sci. Technol. 2021, 1–15.
[54] Lindsley, W.G.; Blachere, F.M.; Beezhold, D.H.; Thewlis, R.E.; Noorbakhsh, B.; Othumpangat, S.; Goldsmith, W.T.; McMillen, C.M.; Andrew, M.E.; Burrell, C.N.; et al. Viable influenza A virus in airborne particles expelled during coughs versus exhalations. Influ. Other Respir. Viruses 2016, 10, 404–413.
[55] Asadi, S.; Wexler, A.S.; Cappa, C.D.; Barreda, S.; Bouvier, N.M.; Ristenpart, W.D. Aerosol emission and superemission during human speech increase with voice loudness. Sci. Rep. 2019, 9, 1–10.
[56] Edwards, D.A.; Ausiello, D.; Salzman, J.; Devlin, T.; Langer, R.; Beddingfield, B.J.; Fears, AC; Doyle-Meyers, L.A.; Redmann, R.K.; Killeen, S.Z.; et al. Exhaled aerosol increases with COVID-19 infection, age, and obesity. Proc. Natl. Acad. Sci. USA 2021, 118, 2021830118.
[57] Heyder, J.; Gebhart, J.; Rudolf, G.; Schiller, C.F.; Stahlhofen, W. Deposition of particles in the human respiratory-tract in the size range 0.005–15 μm. J. Aerosol Sci. 1986, 17, 811–825.
[58] Duguid, J.P. The size and the duration of air-carriage of respiratory droplets and droplet-nuclei. Epidemiol. Infect. 1946, 44, 471–479.
[59] Loudon, R.G.; Roberts, R.M. Droplet expulsion from the respiratory tract. Am. Rev. Respir. Dis. 1967, 95, 435–442.
[60] Papineni, R.S.; Rosenthal, F.S. The Size distribution of droplets in the exhaled breath of healthy human subjects. J. Aerosol Med. 1997, 10, 105–116.
[61] Yan, J.; Grantham, M.; Pantelic, J.; de Mesquita, P.J.B.; Albert, B.; Liu, F.J.; Ehrman, S.; Milton, D.K. Infectious virus in exhaled breath of symptomatic seasonal influenza cases from a college community. Proc. Natl. Acad. Sci. USA 2018, 115, 1081–1086.
[62] Morawska, L.; Johnson, G.; Ristovski, Z.; Hargreaves, M.; Mengersen, K.; Corbett, S.; Chao, C.; Li, Y.; Katoshevski, D. Size distribution and sites of origin of droplets expelled from the human respiratory tract during expiratory activities. J. Aerosol Sci. 2009, 40, 256–269.
[63] Jiang, J.; Fu, Y.V.; Liu, L.; Kulmala, M. Transmission via aerosols: Plausible differences among emerging coronaviruses. Aerosol Sci. Technol. 2020, 54, 865–868.
[64] Spena, A.; Palombi, L.; Corcione, M.; Carestia, M.; Spena, V.A. On the Optimal Indoor Air Conditions for SARS-CoV-2 Inactivation. An Enthalpy-Based Approach. Int. J. Environ. Res. Public Health 2020, 17, 6083.
[65] Spena, A.; Palombi, L.; Corcione, M.; Quintino, A.; Carestia, M.; Spena, VA Predicting SARS-CoV-2 weather-induced seasonal virulence from atmospheric air enthalpy. Int. J. Environ. Res. Public Health 2020, 17, 9059.